Supporting Information for:

Numerical insights on ionic microgels:

structure and swelling behaviour

Giovanni Del Monte,[*,†,‡,¶] Andrea Ninarello,[¶,†] Fabrizio Camerin,[¶,§] Lorenzo

Rovigatti,[†,¶] Nicoletta Gnan,[¶,†] and Emanuela Zaccarelli[*,¶,†]

†*Physics Department, Sapienza University of Rome, Piazzale A. Moro 2 00185 Rome, Italy*

‡*Center for Life NanoScience, Istituto Italiano di Tecnologia, Rome, Italy*

¶*CNR-ISC, Sapienza University of Rome, Piazzale A. Moro 2 00185 Rome, Italy*

§*Department of Basic and Applied Sciences for Engineering, Sapienza University of Rome,*

via A. Scarpa 14, 00161 Rome, Italy

E-mail: giovanni.delmonte@uniroma1.it; emanuela.zaccarelli@cnr.it

S1. Box size effects

It is a known fact that long-range correlations may arise in microgel systems, given the single particle intrinsically inhomogeneous structure in which monomer charges remain fixed, while counterions can freely move throughout the available particle volume. These long-range correlations in the counterion cloud surrounding the particles can strongly affect the microgel swelling properties. In particular, it has been shown that changes in counterions density profile modifies the osmotic pressure balance, causing the deswelling of microgels when the suspension concentration is raised. If this effect happens for neutral microgels in overlapping conditions,[1] for ionic microgel it plays a role already at packing fractions lower than the overlapping ones, though relatively high.[2] In addition, at low packing fractions and highly de-ionised conditions, the hydrodynamic radius has been proven to be strongly concentration-dependent, due to a change in the extension of the external chains, which significantly depends on the amount of the screening from the counterions, in turn determined by their concentration.[2]

Therefore, within our explicit counterions simulations, specific care must be taken to deal with long-range electrostatic interactions. Since we focused our investigation on the study of single particle properties at high dilution, we performed a preliminary analysis on the effects of the choice of the side L of the (cubic) simulation box. Most importantly, we needed to identify a suitable value of L, which was large enough to avoid situations where periodic replicas would be able to feel each other, generating spurious effects.To this aim, we initially performed simulations of a smaller microgel with $N \sim 5000$ monomers with $f = 0.20$ and $c = 3.2\%$, assembled in a spherical cavity of radius $R_0 = 15\sigma$, in different box sizes with $40\sigma \leq L \leq 300\sigma$.

Looking at the variation of the total potential energy per bead E/N, shown in fig. S1, the long-range effects of electrostatic forces are evident, resulting in as a monotonic increase with L, mainly due to the decrease of average couterion concentration. The figure also shows the average bond energy, which remains unaffected by the change in L. Both those effects

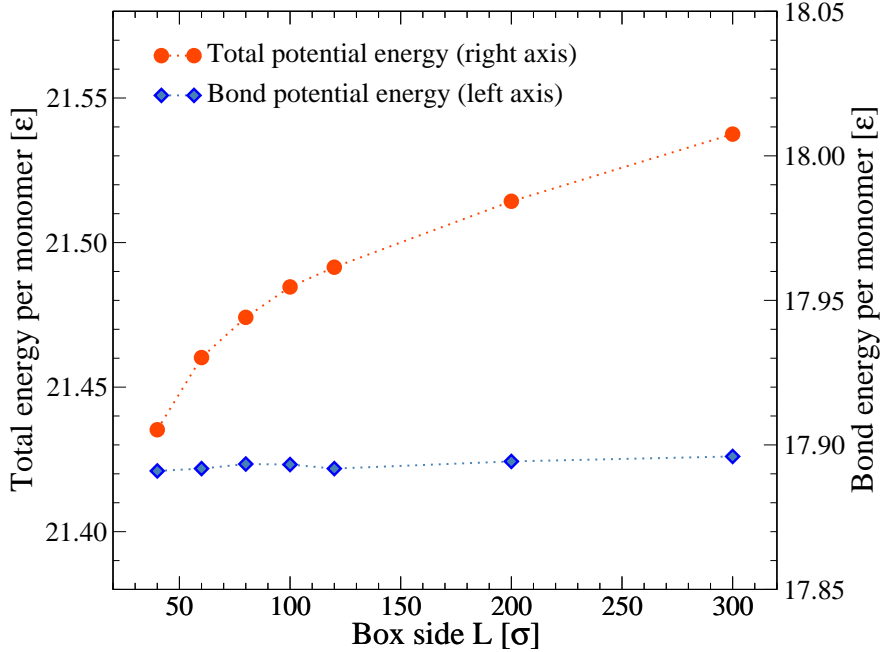are trivial and do not help choosing the correct box side.

Figure S1:   Total potential energy per monomer (scale on the left-axis) and bond potential energy per monomer (scale on the right axis) as a function of the side of the simulation box L. In the latter, only the contribution coming from V_{FENE} is considered.

Relevant insights can be gained by looking at the evolution of the overall dimension and charge of the microgel particle when changing the box size. In Fig. S2 we report the dependence of the gyration radius on the box size. Since this observable mainly takes into account the contribution of the core of the particle, in order to also consider the extent of the corona, we also report the corresponding variation with L of the upper limit of the hydrodynamic radius R^* defined as the radius at which the spatial integral of the monomers density profile is equal to N.[3] Both R_g and R^* do not appreciably vary beyond $L \sim 80\sigma$, suggesting that the size of both the core and the corona of the microgel are stable for large boxes. Similarly, the charge contained inside a sphere of radius R_g, $Q(R_g)$, remains quite constant beyond $L \sim 80\sigma$, while the charge contained in a sphere of radius R^*, $Q(R^*)$, which also accounts for the counterions condensed on the corona of the particle, is found to increase quickly for small values of L and more slowly at high values of L. On the basis of this last result, we select $L = 80\sigma$ as an optimal box size and we thus use the corresponding value
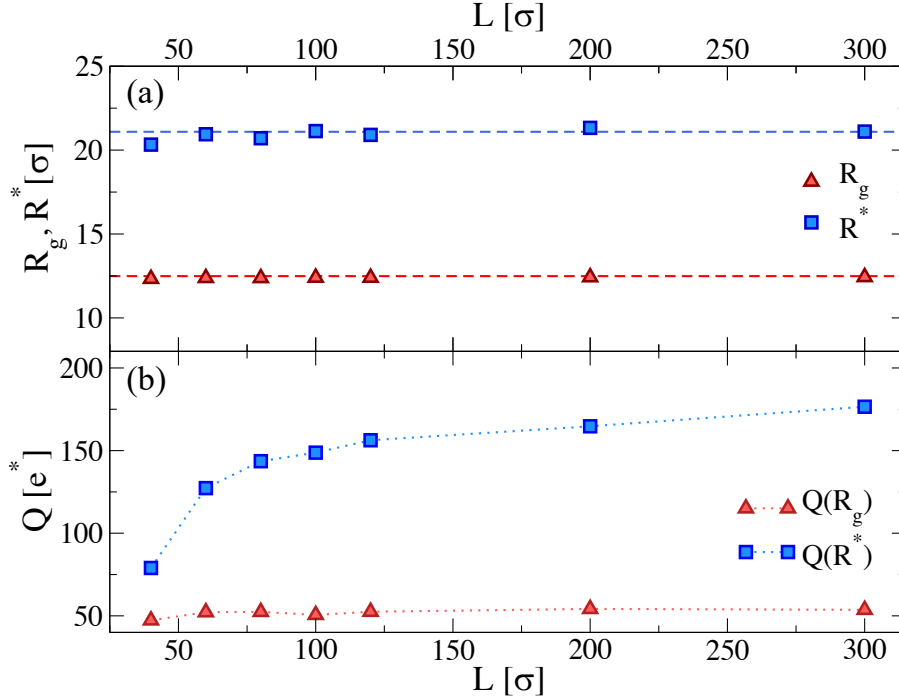
Figure S2: (a) Radius of gyration R_g (triangles) and hydrodynamic radius R^* (squares), defined as in the text, as a function of L; (b) charge contained in a sphere of radius R_g (triangles) and of radius R^* (squares), given in units of e^*, as a function of L.

$L = 300\sigma$ for the larger microgels ($N \approx 42000$) studied in the manuscript.

S2. Choice of the counterion size

We also performed a preliminary analysis on the choice of the counterion size to assess its effects on the microgel properties across the volume phase transition. Clearly, a precise assessment of the coarse-graining size σ_c of counterions, comprehensive of their hydration shell, is not a simple task. In reality, the value of σ_c depends upon the ion species, the temperature, and the local environment wherein the ion is located (if the ion is confined within a dense polymer mesh the structure of its hydration shell could be different than in solution). However from *ab initio* molecular dynamics simulations it is found to be of the order of a few $\mathring{A}$,[4] i.e. sensitively smaller than the Kuhn length of the polymers we are studying. Previous studies[3,5–7] had assigned to counterions the same excluded volume of

monomers. However, we found that such a choice, although having little effect on microgels in the swollen state, dramatically alters their internal structure and swelling properties at high α values. This is due to the fact that, when the solvophobic attraction increases and the microgel shrinks, excluded volume effects become important, so that the counterions become partially trapped in the interior of the microgels, giving rise to an oscillatory charge density profile.

When α increases the polymer beads tend to come in contact with each other in order to minimise the energy. This acts at the same time as the electrostatic attraction between charged monomers and counterions. At sufficiently high α, the solvophobic attraction should win, but if the size of the counterions is too large, the additional steric repulsion will hinder the formation of bead-bead contacts and cause the presence of oscillations in the density profile of both monomers and counterions, as shown Fig. S3. We see that these effects are
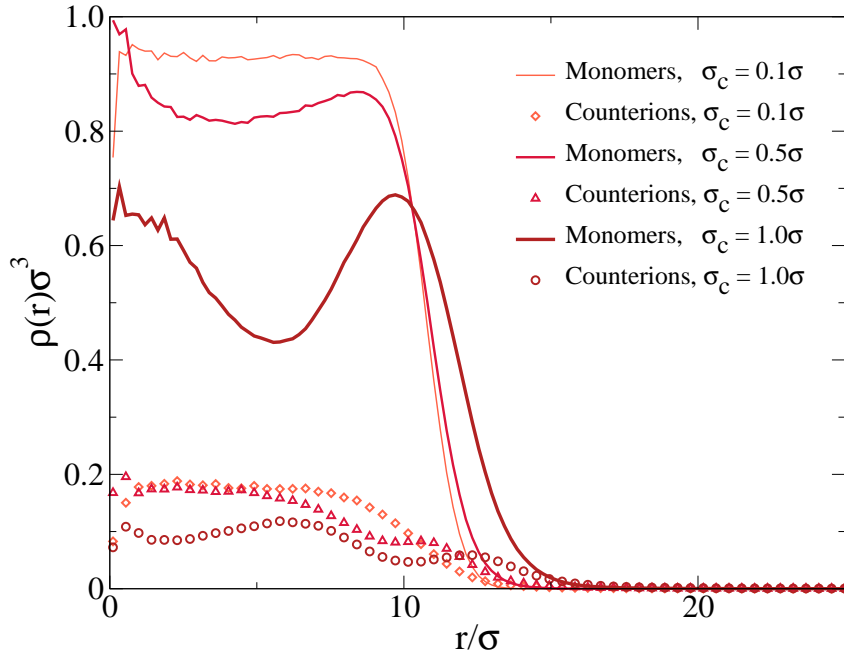

Figure S3: Density profiles of charged monomers (solid lines) and counterions (symbols) for the fully collapsed state ($\alpha = 1.50$) and different sizes of the counterions, i.e. $\sigma_c = 1.0, 0.5, 0.1\sigma$. Data are averaged over 4 different network topologies for microgels with $N \sim 5000$.

very strong for $\sigma_c = \sigma$ and still slightly present for $\sigma_c = 0.5\sigma$, leading to a decrease in the shrinking capability of the microgel at high α values. However, they disappear for $\sigma_c = 0.1\sigma$

that is the counterion size used throughout the manuscript.

S3. Additional details on the form factors fits

In this section we show the form factors of the neutral and Debye-Hückel microgels with $f = 0.20$ at different values of α and we compare them with the fits obtained through the extended fuzzy sphere model with a modified Lorentzian (Eqns. 12 and 13 of the main text). We also comment the evolution of the fits parameters as a function of α and conclude discussing in more detail the capabilities of these models to describe the structure of charged microgels with explicit counterions.

As we can see in Fig. S4, all the data are well described by the model at all studied values of α for both types of microgels. In order to improve statistics, data have been averaged over 4 network topologies.
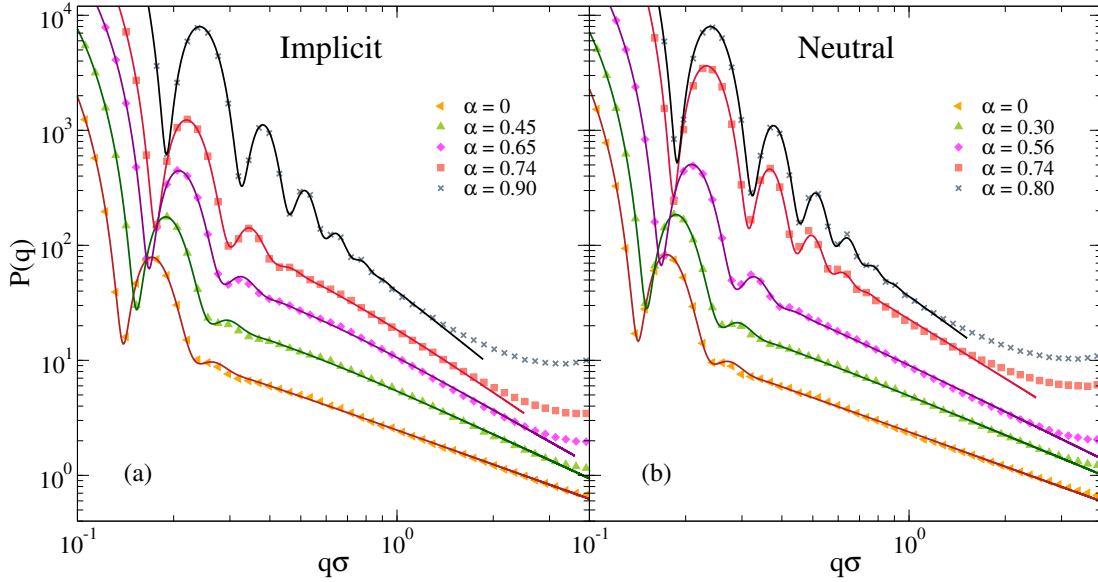

Figure S4: Zoom of the form factors of Figure 9(b,c) of the main text for (a) implicit (DH) and (b) neutral microgels at different values of α. Symbols are simulation data, while lines are fits according to Eqns. 12 and 13 of the main text for $q\sigma \lesssim 3$. Data sets corresponding to the different α values have been vertically shifted for a matter of clarity.

Fig. S5 shows the evolution of the parameters obtained from the fits for the neutral model, the implicit one, and the explicit above the VPT. Panels S5(a,c) display the core radius R and

the surface thickness σ_{surf}, characterising the structure at large length scales, or equivalently in the small-q region of the Fourier space, modelled with and extended fuzzy sphere function (Eq. 12). They both decrease as a function of the effective temperature α, because of the global shrinking of the microgels, as expected. Panels S5(b,d) show the evolution of the
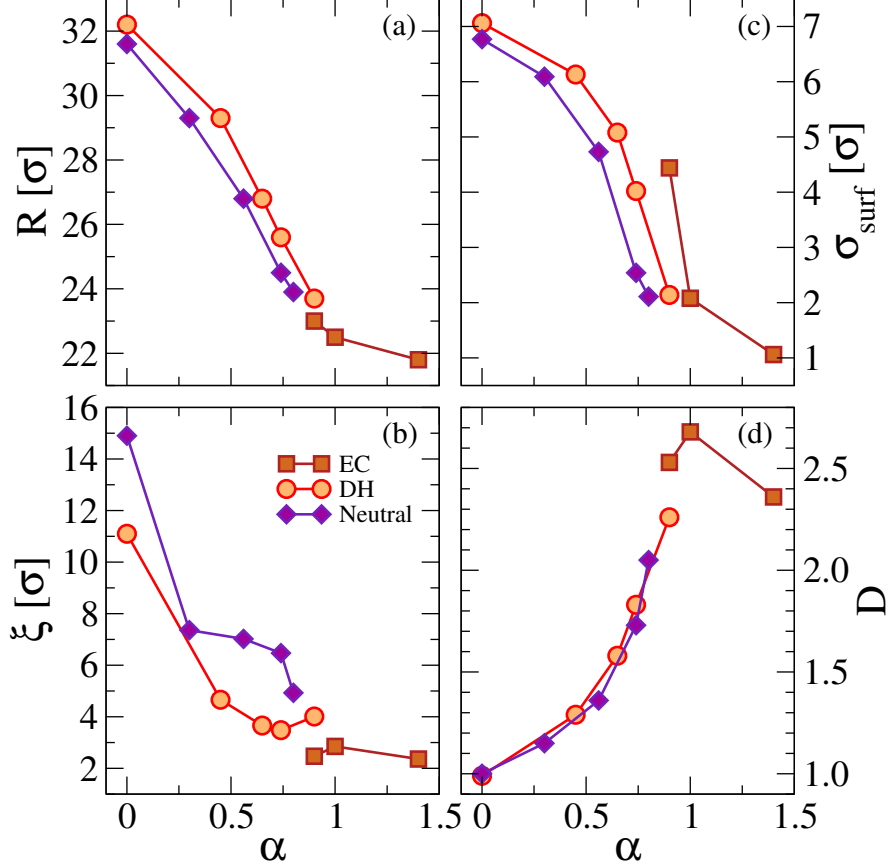

Figure S5: The four panels display the evolution of the fuzzy sphere parameters R and σ_{surf}, the network correlation length ξ and the fractal-dimension exponent D as a function of α, computed by fitting the form factors with Eqns. 12 and 13 of the main text. Three sets of data are shown in each panel: those relative to the microgel with explicit counterions for $\alpha > \alpha_{\mathrm{VPT}}$ (squares), those relative to the Debye-Hückel model (circles), and those relative to the neutral case (diamonds).

correlation length ξ and the fractal dimension exponent D of the Lorentzian contribution (Eq. 13), which accounts for the polymer structure of the network, that is mostly visible in the intermediate- and high-q region. As expected, D increases when increasing α. This indicates the coarsening of the network acted by the solvophobic attraction, which brings close to each other also monomers that are not chemically linked, enhancing the effective connectivity of

the network. The correlation length ξ decreases with increasing temperature, suggesting that the average size of inhomogeneous regions in the polymer networks reasonably decreases when the microgel shrinks, becoming more and more compact and homogeneous. This seems to be also the case for the Debye-Hückel model, showing a qualitative agreement with experimental data,[8] apart from the largest α values, where the errors on these parameters become too large. Indeed the q-range wherein the Lorentzian contribution is found becomes smaller and smaller as α grows, being preempted by the growth of the peaks of the fuzzy sphere. Finally, for $q\sigma \gtrsim 2-3$ the data resolution is limited by the finite size of our numerical model.

When it comes to the microgels with explicit counterions, the modified shape of the corona and the absence of peaks beyond the first one are responsible for the fact that for small values of α a modification of the fitting model must be adopted. We thus only use the modified Lorentzian to fit separately the behavior of the regimes at intermediate q. The resulting fit parameters are summarised in fig. S6 and an extensive discussion of these results is reported in the main text. Here we further notice that finite size effects are responsible for increasing the error on the fit parameters when increasing α. Particularly, for $\alpha = 0.74$ the first flat region of $P(q)$ extends over a too narrow q-interval to get meaningful results for the Lorentzian fit. Hence we constrain the fractal dimension to be close to that observed for smaller values of α, i.e. $D \simeq 0.75$, because it seems to remain constant. This leads us to a value of ξ that is in line with the other α values, that decreases with increasing α. It is also larger for the first Lorentzian function than for the second, in agreement with the interpretation that the structure of the network in the corona (which dominates $P(q)$ at intermediate q values) is more open than that in the core (which dominates $P(q)$ at larger q values).

Above the VPT, the form factors are again well represented by an extended fuzzy sphere model plus a modified Lorentzian, as for the implicit and neutral microgels. These parameters are found in fig. S5. We notice that the Lorentzian parameters of the fit are affected by large errors and their value become very sensitive to the fitting range. This is due to the fact that

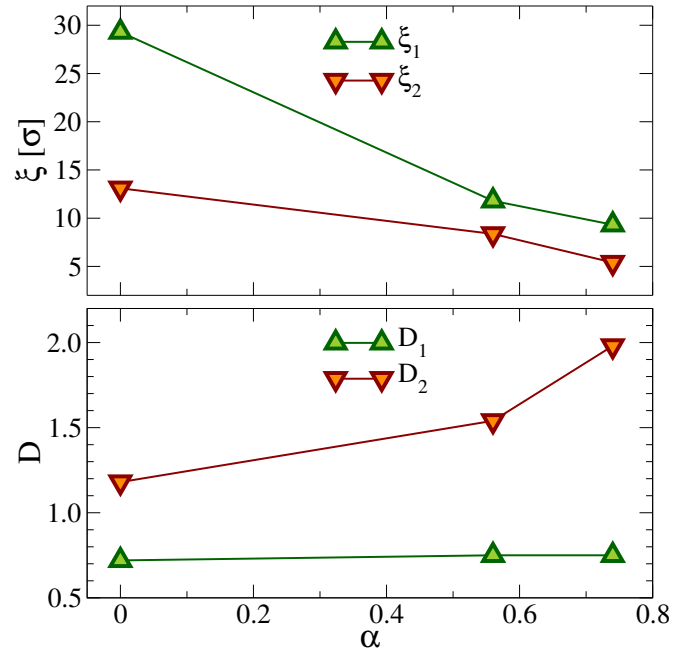the region wherein the Lorentzian contribution dominates $P(q)$ shrinks with increasing α.

Figure S6: Evolution of the network correlation lengths ξ_1 and ξ_2 and of the fractal-dimension exponents D_1 and D_2 as a function of α. The parameters have been extrapolated by fitting the two flat regimes of the form factors of microgels with explicit counterions with a modified Lorentzian function (Eq. 13 of the main text).

References

(1) Mohanty, P. S.; Nöjd, S.; van Gruijthuijsen, K.; Crassous, J. J.; Obiols-Rabasa, M.; Schweins, R.; Stradner, A.; Schurtenberger, P. Interpenetration of polymeric microgels at ultrahigh densities. *Scientific Reports* **2017**, *7*, 1487.

(2) Nöjd, S.; Holmqvist, P.; Boon, N.; Obiols-Rabasa, M.; Mohanty, P. S.; Schweins, R.; Schurtenberger, P. Deswelling behaviour of ionic microgel particles from low to ultrahigh densities. *Soft matter* **2018**, *14*, 4150–4159.

(3) Quesada-Pérez, M.; Maroto-Centeno, J. A.; Martín-Molina, A.; Moncho-Jordá, A. Direct determination of forces between charged nanogels through coarse-grained simulations. *Physical Review E* **2018**, *97*, 042608.

(4) Tuckerman, M.; Laasonen, K.; Sprik, M.; Parrinello, M. Ab initio molecular dynamics simulation of the solvation and transport of hydronium and hydroxyl ions in water. *The Journal of chemical physics* **1995**, *103*, 150–161.

(5) Kobayashi, H.; Halver, R.; Sutmann, G.; Winkler, R. G. Polymer conformations in ionic microgels in the presence of salt: Theoretical and mesoscale simulation results. *Polymers* **2017**, *9*, 15.

(6) Hofzumahaus, C.; Hebbeker, P.; Schneider, S. Monte Carlo simulations of weak polyelectrolyte microgels: PH-dependence of conformation and ionization. *Soft Matter* **2018**, *14*.

(7) Sean, D.; Landsgesell, J.; Holm, C. Computer Simulations of Static and Dynamical Properties of Weak Polyelectrolyte Nanogels in Salty Solutions. *Gels* **2018**, *4*, 2.

(8) Nigro, V.; Angelini, R.; Bertoldo, M.; Bruni, F.; Ricci, M. A.; Ruzicka, B. Dynamical behavior of microgels of interpenetrated polymer networks. *Soft matter* **2017**, *13*, 5185–5193.